

Scaling of the Surface Plasmon Resonance in Gold and Silver Dimers Probed by EELS

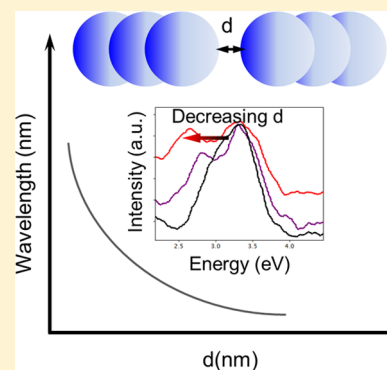
Shima Kadkhodazadeh,^{*,†} Jakob Rosenkrantz de Lasson,[‡] Marco Beleggia,[†] Harald Kneipp,[§] Jakob Birkedal Wagner,[†] and Katrin Kneipp[§]

[†]Center for Electron Nanoscopy, Technical University of Denmark, Kgs. Lyngby, Denmark

[‡]Department of Photonics Engineering, Technical University of Denmark, Kgs. Lyngby, Denmark

[§]Department of Physics, Technical University of Denmark, Kgs. Lyngby, Denmark

ABSTRACT: The dependence of surface plasmon coupling on the distance between two nanoparticles (dimer) is the basis of nanometrology tools such as plasmon rulers. Application of these nanometric rulers requires an accurate description of the scaling of the surface plasmon resonance (SPR) wavelength with distance. Here, we have applied electron energy-loss spectroscopy (EELS) and scanning transmission electron microscopy (STEM) imaging to investigate the relationship between the SPR wavelength of gold and silver nanosphere dimers (radius R) and interparticle distance (d) in the range $0.1R < d < R$. The choice of EELS enables probing the SPRs of individual dimers, whose dimensions and separation distances are measured *in situ* with subnanometer resolution using STEM. We find that the decaying exponential description of the fractional SPR wavelength shift with $d/2R$ holds valid only over a limited range of d . Instead, within the range $0.1R < d < R$ the fractional SPR wavelength shift is found to be related to $(2R/d)^n$, with $n \sim 0.9$ determined for both gold and silver dimers. Despite this common power dependence, consistently larger SPR wavelength shifts are registered for silver for a given change in d , implying silver dimers to be more sensitive plasmon rulers than their gold counterparts.



INTRODUCTION

Plasmonic noble metal nanoparticles are of fundamental interest and play a key role in several technological fields such as ultrasensitive biosensing, nanomedicine, and nanophotonics.^{1–4} This is due to the ability of these nanoparticles to support surface plasmon resonances (SPRs) in the optical range of the electromagnetic spectrum, resulting in the confinement of optical fields to subwavelength dimensions and enhancement of their intensities by several orders of magnitude.⁴ Besides the enhancement and confinement of optical fields, the SPR energy itself is a key parameter in developing new methodologies for ultrasensitive sensing and measuring on the nanometer scale. While the SPR energy of individual nanoparticles can be manipulated, for example through controlling their shape, size, or dielectric environment, an even more impressive phenomenon is how SPRs interact and shift as multiple particles are brought closer together. An example where the tunability of SPR energy with interparticle distance has been explored is in plasmon rulers, in which the recorded shift in SPR energy is used for distance measurement in biological and chemical systems.^{5–7} Advantages of plasmon rulers over other biosensing techniques traditionally used for distance measurement, such as fluorescence resonance energy transfer (FRET), include longer distance detection range, improved sensitivity, and photostability.⁶ It is envisaged that plasmonic rulers can act as sensitive optical sensing tools in cases where certain targets induce an actuation of nanoparticles, and examples of sensing

different chemical and biological activities by them have been demonstrated.^{8–10}

One challenge in successful implementation of plasmonic rulers is accurate calibration of them. Several reports on the scaling of SPR shift with interparticle distance can be found in the literature. A cubic dependence of the dipolar interaction on the inverse of the interparticle distance in chains of nanoparticles is known.¹¹ However, at closer range distances higher order interactions become increasingly important, resulting in deviations from this cubic dependence, with a close to inverse relationship found between the SPR shift and interparticle distance theoretically.^{12,13} Several experimental studies on arrays of gold nanoparticle dimers fabricated by electron lithography have reported an approximately exponential decaying behavior of the SPR wavelength shift with interparticle distance.^{7,14–16} The systematic measurements carried out by Jain et al.⁷ on gold nanodisk dimers together with their discrete dipole approximation (DDA) calculations suggested an exponential expression for the relationship with a decay constant of ~ 0.2 , claimed to be universal, i.e., independent of particle shape, size, composition, and dielectric properties of the surrounding environment. However, the universality of this relationship has been disputed in the literature, with various

Received: January 10, 2014

Revised: February 20, 2014

Published: February 21, 2014

theoretical studies discussing size, shape, and distance dependence of the SPR wavelength shift.^{16–18} In addition, an exponential relationship with a different decay constant has been determined experimentally between the SPR shift of silver nanoparticle dimers in solution and interparticle distance.¹⁹

Electron microscopy has been imperative in most experimental studies of the plasmon ruler nanostructures, and scanning electron microscopy (SEM) or transmission electron microscopy (TEM) has typically been employed pre- or postoptical measurements in order to accurately determine dimensions and distances.^{7,14,19} This is due to the limited spatial resolution of optical techniques (at best a few tens of nanometers), which is typically insufficient to accurately measure the dimensions and distances in plasmonic structures. Besides being a tool for high resolution imaging, the electron beam in a TEM can also be used to excite surface plasmons and study their properties with electron energy-loss spectroscopy (EELS).^{20–23} While this has been known for a long time, it is only in recent years that the application of EELS is extended to the visible light energy range and below (due to improvements in the energy resolution of modern TEM instruments), providing the opportunity to perform simultaneous imaging and spectroscopy on plasmonic structures in a TEM with subnanometer spatial resolution. Moreover, the limited spatial resolution of optical techniques has meant that many studies of the scaling of SPR in plasmon rulers have relied on measurements on ensemble structures fabricated by electron lithography instead of probing individual structures. Depending on the accuracy of electron beam lithography, statistical variation in interparticle separation, shape, or size of the fabricated structures occurs, leading to the measurement of an averaged optical response of the ensemble. Here we have applied scanning TEM (STEM) imaging combined with EELS to accurately determine and compare the scaling of the SPR energy with interparticle distance in (quasi-) spherical gold and silver dimers. The high spatial resolution of EELS allows these measurements to be recorded from individual dimers instead of ensembles. Moreover, in several cases the particles could be moved *in situ* relative to each other by electron-beam-induced forces, allowing measurements to be taken from the same dimer at different separations.

The experimental results are interpreted on the basis of three-dimensional and fully retarded optical scattering calculations of gold and silver nanosphere dimers. This method is based on a formalism for solving the Lippmann–Schwinger equation of the electric field in three dimensions. While the DDA method, applied for example by Jain et al.,⁷ is a versatile means for solving the volume integral equation for the electric field and can be applied to arbitrarily shaped scatterers, typically a very large number of discrete dipoles are required to obtain accurate results. In contrast, the multiple scattering method applied here produces a much smaller system of equations to solve, simplified by exploiting the spherical symmetry of the scatterers analyzed (as demonstrated in detail elsewhere²⁴), and thus produces more accurate results for this particular geometry.

■ EXPERIMENTAL AND COMPUTATIONAL METHODS

Particle Preparation. Silver nanoparticles were prepared by laser ablation from bulk silver in water using 532 nm laser pulses with pulse lengths of 10 ns, a repetition rate of 10 Hz, and pulse energies of ~ 0.15 W·s. Gold nanoparticles were

prepared from gold chloride in a chemical reduction process using sodium citrate.

Electron Microscopy and EELS. TEM specimens were prepared by depositing the solution containing the nanoparticles on a 5 nm thick amorphous Si_3N_4 membrane followed by evaporation. EELS measurements were carried out in STEM mode using a monochromated FEI Titan instrument operated at 120 kV. Spatial and energy resolution of the measurements were 0.4 nm and 0.15 eV, respectively. Energy dispersion per channel of 0.01 eV and acquisition time of 0.1–0.2 s per spectrum were used. STEM images of dimers were recorded before and after the EELS acquisitions and were used to measure dimensions and distances between particles. Spectra were analyzed after removing the zero-loss peak and the background post-plasmon features due to the substrate. SPR energies were determined by least-squares fitting the plasmon features (both bright and dark modes) with Gaussian functions.

Multiple Scattering Simulations. Fully retarded calculations based on a volume integral equation and the dyadic Green's function for the electric field were used to simulate the extinction efficiency of nanosphere dimers with radii R and interparticle distance d , immersed in a homogeneous background medium illuminated with light polarized along the dimer axis and energy in range 0.5–5.0 eV. SPR energies were retrieved as the peaks in the extinction spectra for interparticle separation distance range $0.1R < d < 2R$. The dielectric functions of gold and silver particles are obtained from the Lorentz–Drude model that takes inter- and intraband transitions in metals into account.²⁵ The presence of a substrate in the experimental measurements was accounted for in the simulations by determining an effective permittivity (ϵ_{eff}) value for the environment around the particles. The effective permittivity was determined as the background permittivity in the simulations that yields the same experimental and calculated value of the SPR energy for isolated nanoparticles. This effective permittivity value ($\epsilon_{\text{eff}} = 1.25$ for silver and 1.35 for gold) was then used to simulate the extinction efficiency of dimers. As discussed in detail by de Lasson et al.,²⁴ within a local description and neglecting quantum effects, the optical scattering calculations are only limited by the truncation of the series expansions of the electric fields over the spherical harmonic functions of order l , where the sum is truncated at a finite l_{max} . For all structures an $l_{\text{max}} = 8$, giving a global relative error on the calculated electric field of $\sim 1\%$, was used as a starting point. If the SPR energies obtained with $l_{\text{max}} = 8$ and $l_{\text{max}} = 9$ did not converge, l_{max} was increased. Only in instances $d < 0.3R$, a higher l_{max} than 8 was required to obtain converged values of the SPR energy. More details on the calculations, including validation of the method, can be found elsewhere.²⁴

Since the calculations are specific to the scenario where the dimers are illuminated by an electromagnetic (light) plane-wave polarized along the axis, while in the experiments plasmons are generated by the electric field of a moving electron, swiftly passing by and losing energy in the process, and such electric field differs greatly from the uniform harmonic field of polarized light, a question may arise as to whether the SPR scaling calibration performed with electrons is significant to plasmon rulers excited and probed by photons. The issue of electron vs photon plasmonic excitations has recently been discussed by Collins and Midgley,²⁶ who demonstrated by means of explicit calculations that the positions of modal maxima (i.e., in our case, the SPR peak position) are the same regardless of whether electrons or photons were used to excite them. It is, instead, the

probability of exciting particular modes (the Mie expansion coefficients, determined by boundary conditions, which, in turn, are obviously different for plane-wave polarized light and for a moving charge) that depends on the chosen irradiation. The various plasmonic modes that can exist in a given system are, in fact, exclusively dependent on the geometry (shape, size, separation, environment, etc.), and using photons or electrons only affects which modes are excited. The primary example of this is the so-called “dark mode”, which can be excited with electrons but not with polarized light.

RESULTS AND DISCUSSION

STEM and EELS Measurements of Dimers. Measurements were taken from different sets of dimers with radii (R , see inset in Figure 3d) $13 \text{ nm} < R < 19 \text{ nm}$ in gold particles and $9 \text{ nm} < R < 15 \text{ nm}$ in silver particles. Only dimers with particles of similar dimensions and with shapes close to spherical were selected for analysis. Furthermore, only surface to surface interparticle distances $d > 0.1R$ (see inset in Figure 3d) are considered here, since nonlocal and quantum effects are not expected to play a significant role in this range.^{27–29} However, it is worth emphasizing that data points could be acquired at even smaller separations,²⁹ further extending the investigation of the SPR scaling law in a range where dimers are in very close proximity, a regime which is very difficult to access both theoretically and experimentally with non-STEM techniques.

As discussed in detail by Batson et al.,³⁰ the interaction between the electron beam and a pair of nanoparticles in STEM can result in both attractive and repulsive forces (depending on the location and direction of scanning) and induce movement of the particles. Figure 1 shows an example

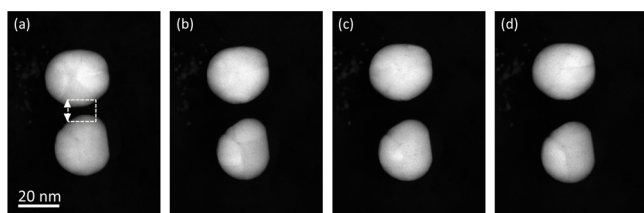


Figure 1. STEM images of a pair of gold nanoparticles moved relative to each other by scanning the electron probe for 2–3 min in the area between the particles, similar to the dotted box in (a) and with the scanning direction along the marked arrows, i.e., perpendicular to the long axis of the particles. The surface to surface distance between the particles in (a)–(d) are approximately 4.0, 7.4, 9.2, and 10.7 nm, respectively.

in which a repulsive force was induced between two particles by scanning the electron probe in the gap between the particles, resulting in movement of the particles relative to each other and increasing their separation. This phenomenon could be used in several cases to modify the distance between the particles and to record the SPR energies of the same dimer separated at different distances.

Example STEM images of the gold and silver dimers are displayed in Figures 2a and 2c. The respective EEL spectra of the dimers, with the electron beam placed in the periphery (at the position of the dots in each image), are displayed in Figures 2b and 2d. As discussed by Koh et al.,²² EELS probes the bright dipolar and dark SPRs of a dimer when the electron beam is in the periphery of the structure. The bright dipolar SPR in this case corresponds to the optically excited mode with the light

polarization along the long axis of the dimer. It is the energy of this plasmon mode that is monitored for sensing in plasmon ruler structures, and our EELS measurements and simulations here follow the relationship between this parameter and interparticle distance.

Scaling of SPR Wavelength Shift with Interparticle Distance. The EELS measurements and optical scattering calculations of the SPR energies (E_p) of gold and silver dimers as functions of the ratio surface to surface distance to particle diameter $x = d/2R$ are plotted in Figures 3a and 3b. The error bars in the experimental measurements of x correspond to the spatial resolution limit of determining d and R ($\pm 0.4 \text{ nm}$), but the deviation of the profiles of the particles in STEM images (projected through the thickness of the particles) from perfect circles and the difference in the sizes of the two particles forming a dimer are not included. The error bars in E_p correspond to the uncertainty in the measurements arising primarily from the overlap between the bright dipolar mode and the dark mode in the EEL spectra at larger interparticle distances, plus the noise present in the data. Overall, a very good agreement is seen between the EELS measurements and the simulations, confirming that the same SPR modes are excited both optically and with an electron beam. The simulated E_p vs x plots show very little dependence on particle radius R within the range considered, indicating that differences in the radii of the dimers studied experimentally may be neglected in the analyses. Moreover, the good agreement between the experimental and simulations suggests that reasonably small deviations in the shape of the particles from perfect spheres or small differences in the radii of the two particles forming dimers do not affect the SPR energy significantly and can be neglected here.

Most studies of the SPR scaling law have considered the fractional shift ratio in resonance wavelength $\Delta\lambda/\lambda_0 = (\lambda - \lambda_0)/\lambda_0$ as a function of $d/2R$, where λ is the SPR wavelength of a dimer and λ_0 the SPR wavelength of a single particle of the same radius. Accordingly, plots of $y = \Delta\lambda/\lambda_0$ versus $x = d/2R$ of our EELS and simulated data on gold and silver dimers are shown in Figures 3c and 3d, respectively.

In order to ascertain whether an exponential function can adequately describe the fractional shift ratio, semilogarithmic plots $\log(y)$ vs x along with the least-squares exponential fits through the experimental data and their corresponding R^2 values are displayed in Figures 4a and 4c. Very similar least-squares exponential fits to the universal exponential function suggested by Jain et al.⁷ are determined here, with a decay constant of ~ 0.2 found for both gold and silver dimers. However, these semilogarithmic plots do not appear particularly linear, despite the reasonable R^2 values of these exponential fits. In particular, the slope of the plots deviate from the suggested universal value of 0.2, at the lower and higher ends of the range considered ($0.1R < d < R$). A more appropriate test for the quality of these exponential fits can be determining the errors associated with estimating d from y values, as is the primary purpose of plasmon rulers. In this case, errors as large as $\sim 50\%$ are found when estimating distances at either ends of the range studied (i.e., $d \sim 0.1R$ or $d \sim R$) using the exponential SPR scaling relationship.

Power law functions of the form Ax^{-n} are found to provide improved estimates of $y(x)$, as is clear from the corresponding log–log plots of the data in Figures 4b and 4d. Approximately the same power dependence $n \sim 0.9$ is determined for both gold and silver. In contrast to an exponential decay estimation,

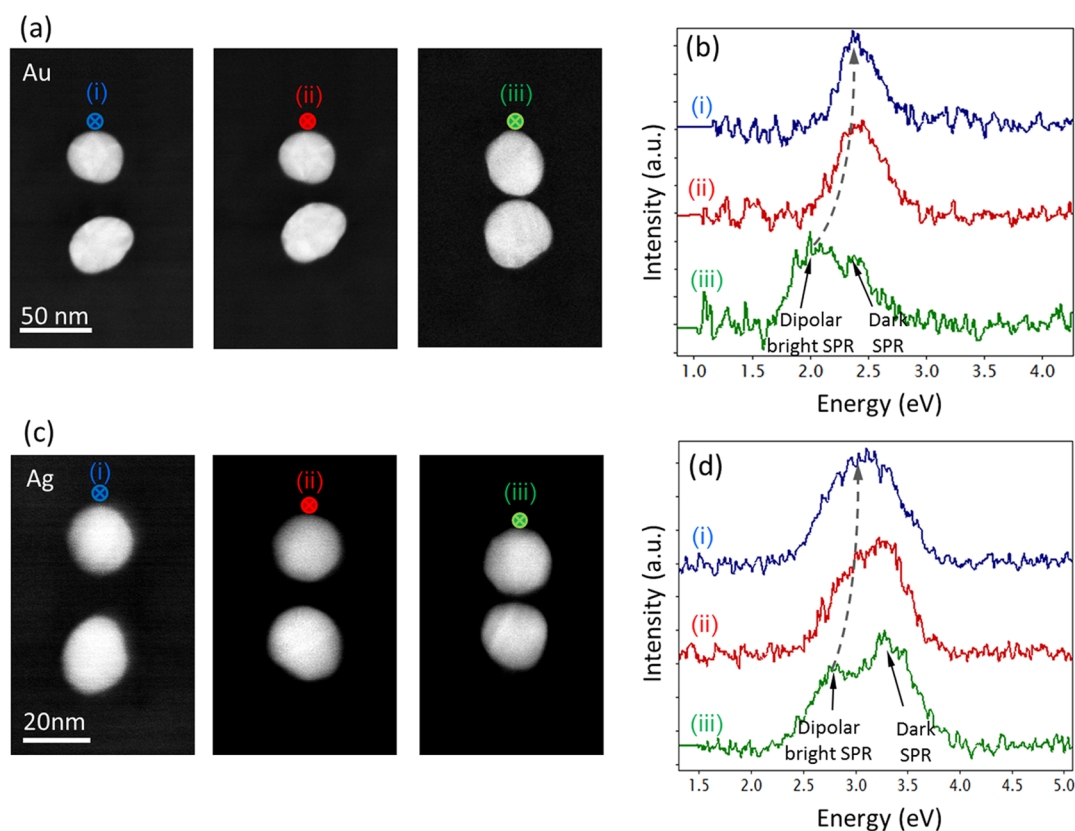


Figure 2. STEM images of (a) gold (Au) and (c) silver (Ag) dimers with different separation distances. (b, d) The corresponding EEL spectra of the dimers in (a) and (c). The dots in STEM images denote the position of the electron beam in each measurement.

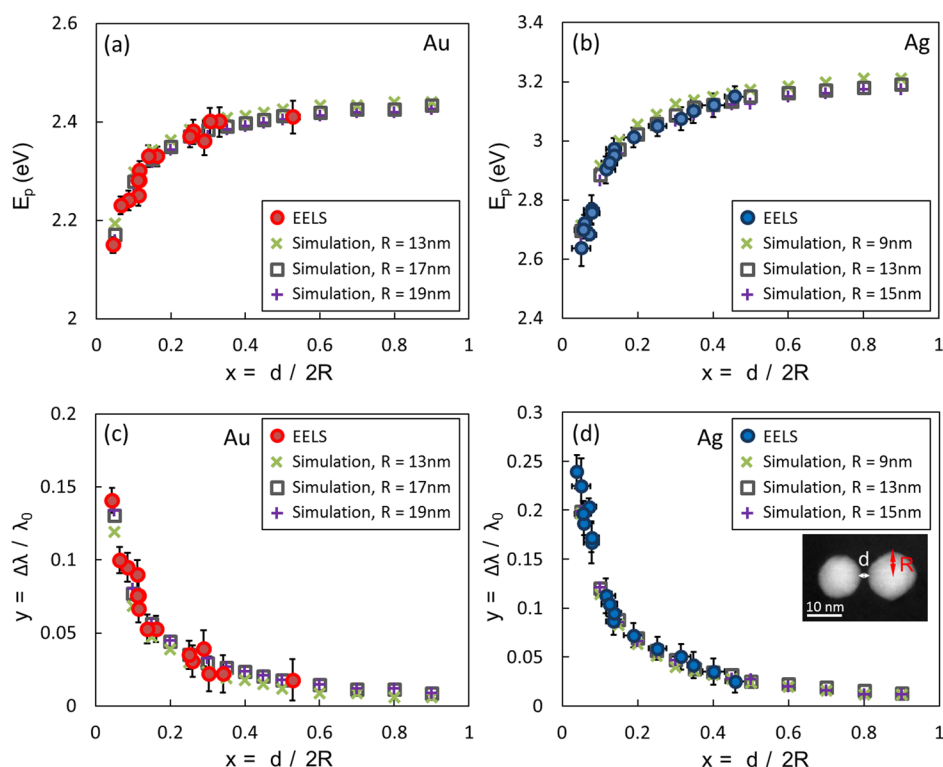


Figure 3. SPR energies (E_p) measured with EELS and simulated for (a) gold and (b) silver dimers as functions of the ratio $x = d/2R$ (see inset in (d)). The experimentally measured and simulated fractional SPR wavelength shift ratios $y = \Delta\lambda/\lambda_0$ as functions of x in (c) gold and (d) silver dimers.

this power law relationship appears valid over the entire interparticle distance range considered here, with at most errors

$\sim 14\%$ associated with estimating d from y . Harris et al.¹³ have reported very similar results based on their calculations of the

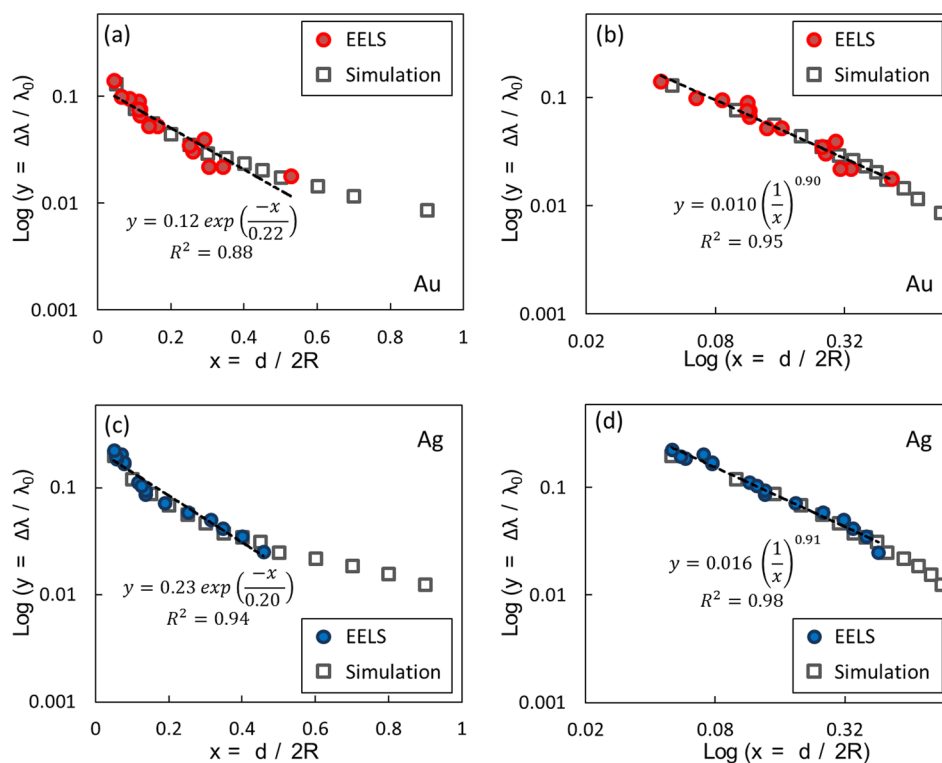


Figure 4. (a, c) Semilogarithmic scale and (b, d) logarithmic scale plots of the experimentally measured and simulated ($R = 17$ nm for gold and $R = 13$ nm for silver) fractional SPR wavelength shift ratios $y = \Delta\lambda/\lambda_0$ of (a, b) gold and (c, d) silver dimers as functions of $x = d/2R$. The exponential and power law fits found for the experimental data along with their corresponding R^2 values are also stated in each case.

SPR wavelength in closely coupled gold nanosphere chains using the T-matrix method, giving $n = 0.89$ for dimers. This power dependence is considerably different from the expected inverse cubic relationship for classical dipolar coupling. The inverse cubic relationship, derived for point dipoles,³¹ has been shown theoretically to be valid only at longer range distances, where the distance between particles exceeds their size ($d > R$).³² However, within the distance range considered here ($d < R$), as typically also relevant to plasmon rulers, the interaction between two particles deviates considerably from that of classical dipoles. As explained by Nordlander et al.³³ based on the plasmon hybridization model, in dimers the $l = 1$ dipole mode of one particle begins to interact and mix with the $l' > 1$ multipole modes of the other particle. As a result, the hybridized plasmon SPR is expected to scale with distance proportional to $L^{-(l+l'+1)}$, where $L = d + 2R$ is the center-to-center distance between the two particles in the dimer. At close range distances, higher order multipoles become dominant, resulting in a stronger red-shift of the dipolar SPR with interparticle distance than that expected from a purely dipolar interaction. This change in the coupling behavior of particles in short- and long-range distances can be readily seen in our logarithmic scale plots of y versus $L/2R$. As shown in Figure 5, y scales approximately with $(L/2R)^{-3}$ for $L \sim 4R$ (corresponding to $d \sim 2R$), implying a classical dipolar behavior in this range ($l = 1, l' = 1$, hence $L^{-(l+l'+1)} = L^{-3}$). However, as the separation between the particles decreases, the fractional SPR wavelength shift increases more and more rapidly, becoming proportional to $(L/2R)^{-9}$ for $L \sim 2.2R$ (corresponding to $d \sim 0.2R$), suggesting that as the separation decreases we capture progressively the contributions from quadrupole–quadrupole interactions ($l = 2, l' = 2$, hence $L^{-(l+l'+1)} = L^{-5}$) and higher modes up to the sextupole–sextupole ($l = 4, l' = 4$, hence L^{-9}).

The graphs in Figure 5 can be closely approximated to rational functions of the form $f(L/2R) = p/[\sum_{n=0}^N q_n (L/2R)^n]$, where p, q_n , and N are constants and the $q_n (L/2R)^n$ terms arise from the decaying behavior of the hybridized plasmon mode with distance. The values of the coefficients q_n are such that within the range $2R < L < 3R$ (corresponding to $d < R$) the function $f(L/2R) = \Delta\lambda/\lambda_0$ becomes approximately proportional to $(L/2R - 1)^{-1}$ or $(d/2R)^{-1}$. This behavior can be explained in an intuitive way using the optical nanocircuit model.^{34,35} Figure 6 shows the equivalent nanocircuit for two noble metal nanospheres separated at distance $d < R$, illuminated by an electromagnetic plane-wave with frequency ω in the visible light range, as proposed by Alu et al.^{34,35} The components L_s, C_p and C_g correspond to the nanocircuit elements describing the electric field induced inside the noble metal nanospheres (inductive), the fringe dipolar electric field outside the nanospheres (capacitive), and the gap between the particles (capacitive), respectively.^{34,35}

The corresponding impedances of these components have been estimated as $Z_{L_s} = (-i\omega R\pi\text{Re}[\epsilon])^{-1}$, $Z_{C_p} = (-i\omega 2\pi R\epsilon_0)^{-1}$, and $Z_{C_g} = (-i\omega C_g)^{-1}$, where ϵ_0 is the permittivity of the medium around the particles and $\epsilon(\omega)$ is the permittivity of the noble metal nanoparticles are made of.^{34,35} Using these expressions, we derive the total impedance of the nanocircuit in Figure 6, $Z_{\text{total}} = (2Z_{L_s}Z_{C_p})/(Z_{L_s} + Z_{C_p}) + Z_{C_g}$ to be

$$Z_{\text{total}} = \frac{2C_g + \pi R(2\epsilon_0 + \text{Re}[\epsilon])}{j\omega\pi RC_g(2\epsilon_0 + \text{Re}[\epsilon])} \quad (1)$$

Excitation of the dipolar mode requires $Z_{\text{total}} = 0$. This gives the condition for resonance in a nanosphere dimer as

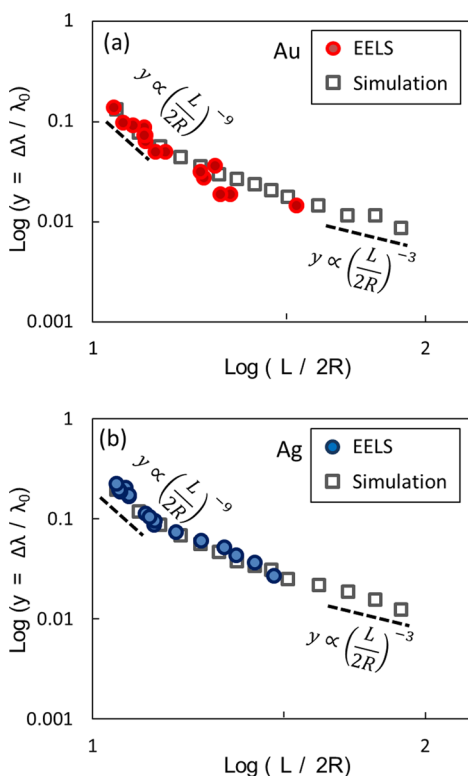


Figure 5. Logarithmic scale plots of the experimentally measured and simulated ($R = 17$ nm for gold and $R = 13$ nm for silver) fractional SPR wavelength shift ratios $y = (\Delta\lambda/\lambda_0)$ of (a) gold and (b) silver dimers as functions of $L/2R$, where $L = d + 2R$ is the center-to-center distance between the spheres in the dimer. The dashed lines show how the scaling of y with $L/2R$ changes at short- and long-range distances.

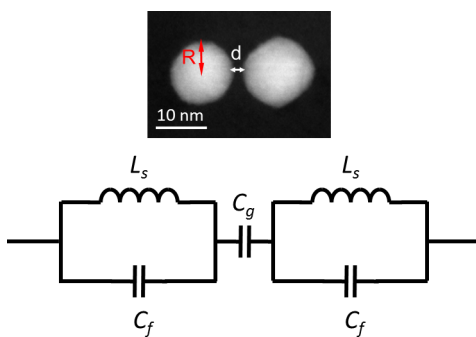


Figure 6. Equivalent nanocircuit of two closely spaced noble metal nanospheres illuminated by an electromagnetic plane-wave of frequency in the visible light range.³⁵ In the case of noble metals where $\text{Re}[\epsilon] < 0$, the nanospheres are modeled as inductors L_s , the fringe field outside the particles as capacitors C_f , and the gap between the particles as a capacitor C_g .

$$\text{Re}[\epsilon] = -\frac{2C_g}{\pi R} - 2\epsilon_0 \quad (2)$$

For very large interparticle distances, $d \rightarrow \infty$, the capacitance in the gap between the particles tends to zero, resulting in the well-known condition for SPR in a single sphere, $\text{Re}[\epsilon] = -2\epsilon_0$. Utilizing the approximately linear relationship between $\text{Re}[\epsilon]$ and wavelength λ in the visible light range in gold and silver, $\lambda = p - q\text{Re}[\epsilon]$, where $\lambda = 463 - 14.5\text{Re}[\epsilon]$ in the case of gold and $\lambda = 318 - 18.5\text{Re}[\epsilon]$ in the case of silver,³⁶ in combination with eq 2, the SPR wavelength in dimers can be written as

$$\lambda = p + 2q \left(\frac{C_g}{\pi R} + \epsilon_0 \right) \quad (3)$$

Using eq 3 together with the resonance condition in single gold and silver spheres, the fractional SPR wavelength shift ($\Delta\lambda/\lambda_0$) in closely spaced dimers is derived as

$$\frac{\Delta\lambda}{\lambda_0} = \frac{\lambda - \lambda_0}{\lambda_0} = \frac{2q \left(\frac{C_g}{\pi R} \right)}{p + 2q\epsilon_0} \quad (4)$$

Alu and Engheta³⁵ have estimated the gap capacitance in nanosphere dimers as $C_g = \epsilon_0\pi R^2/d$, where charge distribution over half the surface area of spheres is assumed. Using this capacitance relationship, the p and q values for gold and silver and their respective effective permittivities employed in our multiple scattering calculations, eq 4 gives $\Delta\lambda_{\text{Au}}/\lambda_0 = 0.039(d/2R)^{-1}$ in the case of gold and $\Delta\lambda_{\text{Ag}}/\lambda_0 = 0.064(d/2R)^{-1}$ in the case of silver. While here we have demonstrated the near-inverse relationship between $\Delta\lambda/\lambda_0$ and $d/2R$ as was found experimentally, higher amplitudes are determined based on the nanocircuit model than the experimental values (see Figure 4). We attribute this difference to the surface charge distribution (and hence the capacitance) in two closely spaced nanoparticles differing from that assumed by Alu and Engheta.³⁵ As the distance between nanoparticles decreases, the effective surface area where charge accumulates becomes increasingly localized (i.e., smaller). This is analogous to and follows on from the increasing importance of multipolar interactions between the particles at smaller separation distances, as discussed earlier. Comparing the amplitudes determined from the nanocircuit model to those found from the experimental results suggests a factor of 4 smaller effective surface area charge distribution than the assumed semispherical surface area (see Figure 7).

Comparison between Gold and Silver. While the results so far reveal common parameters between gold and silver dimers in both the exponential and power law estimates of their fractional SPR shift scaling with distance, consistently larger amplitudes are inferred for the fractional SPR shift in silver than gold. In order to comment on any superiority in sensitivity of one material over the other as plasmon rulers, $\Delta\lambda = \lambda - \lambda_0$ determined for gold and silver dimers are compared in Figure 8. The results show that consistently larger $\Delta\lambda$ values are registered for a given change in d in the case of silver than gold, in both the EELS measurements and the simulations. This implies that silver plasmon rulers are more sensitive to small changes in interparticle distance than their gold counterparts and hence, as also pointed out elsewhere,^{18,19} can act as more sensitive plasmon rulers.

CONCLUSIONS

In conclusion, we investigated the scaling of the SPR energy of gold and silver nanosphere dimers with radius R and surface to surface separation distance d , using combined STEM imaging and EELS, within the range $0.1R < d < R$. Applying EELS to probe the plasmon response of individual dimers enabled simultaneous spectroscopy and subnanometer resolution measurement of R and d . The results were compared to three-dimensional, fully retarded optical scattering calculations. It was found that exponential relationships similar to the universal function suggested in the literature could only describe the fractional shift in SPR wavelength over a limited range of interparticle distances, as the quality of these

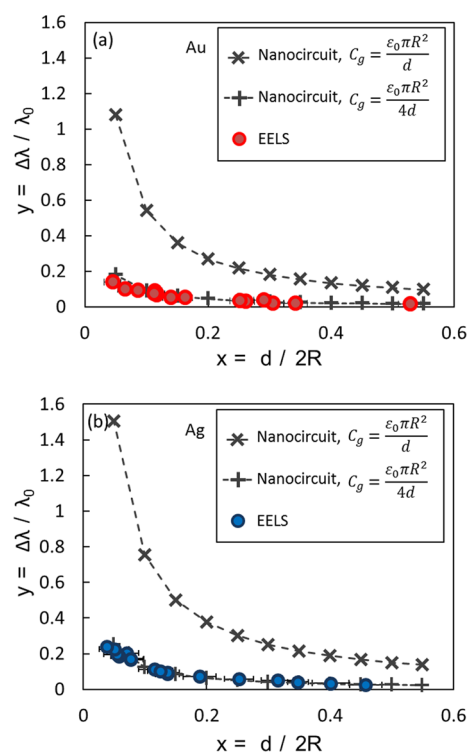


Figure 7. Fractional SPR wavelength shift values $y = \Delta\lambda/\lambda_0$ of (a) gold and (b) silver dimers as functions of $x = d/2R$ measured experimentally and determined from the nanocircuit model for gap capacitance C_g with effective surface area charge distribution equivalent to that of hemisphere and that 4 times smaller, giving respectively $C_g = \varepsilon_0\pi R^2/d$ and $C_g = \varepsilon_0\pi R^2/4d$.

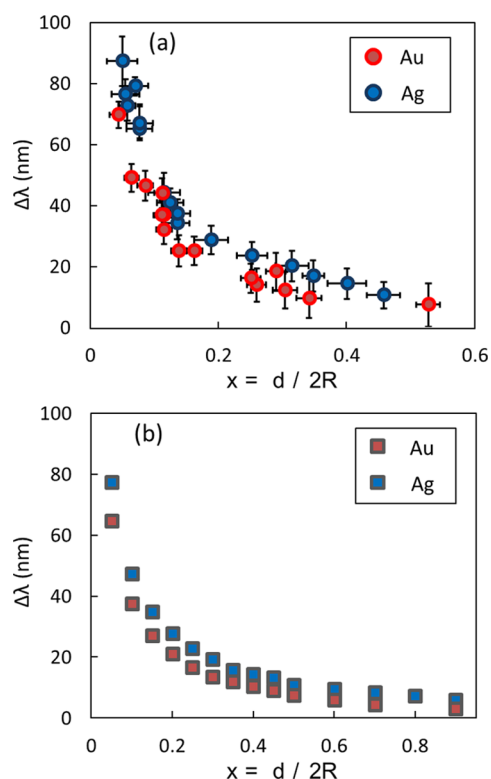


Figure 8. (a) Experimentally measured and (b) the simulated SPR wavelength shift $\Delta\lambda = \lambda - \lambda_0$ in gold and silver dimers as functions of $x = d/2R$.

estimations deteriorated especially at the lower or higher ends of the $d/2R$ range analyzed. The fractional shift in SPR wavelength could instead be related to $(2R/d)^{0.9}$, with the power dependence ~ 0.9 found to be independent of the choice of gold or silver. In contrast to a decaying exponential relationship, this power law relationship was valid over the entire range $0.1R < d < R$. This power dependence, also predicted by the T-matrix modeling of closely coupled gold nanosphere dimers carried out by Harris et al.,¹³ is notably different from the inverse cubic relationship expected in dipolar coupling. Examining the dependence of the fractional SPR wavelength shift on center-to-center interparticle distance ($L = 2R + d$) demonstrated that a dipolar interaction approximation is valid only at large interparticle distances. In close distance range coupling ($d < R$), the fractional SPR wavelength shift was found to scale with a higher order than cube of the inverse (center-to-center) interparticle distance and the power dependence increased for decreasing distances. This provides experimental evidence supporting the validity of the plasmon hybridization model, confirming that multipolar interactions become increasingly important at smaller distances and begin to interact and mix with the dipole mode.³³ Other theoretical studies,^{13,18,32} including our multiple scattering simulations in an earlier publication,²⁴ have also demonstrated the breakdown of a strictly dipolar interaction between nanoparticles with $d < R$. Finally, when comparing gold and silver dimers, the SPR wavelength in silver dimers was found to be more sensitive to changes in d than gold dimers. These results are of interest to and contribute to a better understanding of plasmon rulers.

AUTHOR INFORMATION

Corresponding Author

*E-mail: shka@cen.dtu.dk (S.K.).

Notes

The authors declare no competing financial interest.

ACKNOWLEDGMENTS

The A.P. Møller and Chastine McKinney Møller Foundation is gratefully acknowledged for their contribution towards the establishment of the Centre for Electron Nanoscopy in the Technical University of Denmark.

ABBREVIATIONS

EELS, electron energy-loss spectroscopy; SPR, surface plasmon resonance; TEM, transmission electron microscopy; STEM, scanning transmission electron microscopy.

REFERENCES

- (1) Anker, J. N.; Hall, W. P.; Lyandres, O.; Shah, N. C.; Zhao, J.; Van Duyne, R. P. Biosensing with Plasmonic Nanosensors. *Nat. Mater.* **2008**, *7*, 442–453.
- (2) Kneipp, J.; Kneipp, H.; Wittig, B.; Kneipp, K. Novel Optical Nanosensors for Probing and Imaging Live Cells. *Nanomed. Nanotechnol. Biol. Med.* **2010**, *6*, 214–226.
- (3) Gramotnev, D. K.; Bozhevolnyi, S. I. Plasmonics beyond the Diffraction Limit. *Nat. Photonics* **2010**, *4*, 83–91.
- (4) Giannini, V.; Fernandez-Dominguez, A. I.; Heck, S. C.; Maier, S. A. Plasmonic Nanoantennas: Fundamentals and Their Use in Controlling the Radiative Properties of Nanoemitters. *Chem. Rev.* **2011**, *111*, 3888–3912.
- (5) Su, K. H.; Wei, Q. H.; Zhang, X.; Mock, J. J.; Smith, D. R.; Schultz, S. Interparticle Coupling Effects on Plasmon Resonances of Nanogold Particles. *Nano Lett.* **2003**, *3*, 1087–1090.

- (6) Reinhard, B. M.; Siu, M.; Agarwal, H.; Alivisatos, A. P.; Liphardt, J. Calibration of Dynamic Molecular Rule Based on Plasmon Coupling between Gold Nanoparticles. *Nano Lett.* **2005**, *5*, 2246–2252.
- (7) Jain, P. K.; Huang, W.; El-Sayed, M. A.; El-Sayed, M. A. On the Universal Scaling Behavior of the Distance Decay of Plasmon Coupling in Metal Nanoparticle Pairs: A Plasmon Ruler Equation. *Nano Lett.* **2007**, *7*, 2080–2088.
- (8) Sonnichsen, C.; Reinhard, B. M.; Liphardt, J.; Alivisatos, A. P. A Molecular Ruler Based on Plasmon Coupling of Single Gold and Silver Nanoparticles. *Nat. Biotechnol.* **2005**, *23*, 741–745.
- (9) Chen, J. I. L.; Chen, Y.; Ginger, D. S. Plasmonic Nanoparticle Dimers for Optical Sensing of DNA in Complex Media. *J. Am. Chem. Soc.* **2010**, *132*, 9600–9601.
- (10) Jun, Y.-W.; Sheikholeslami, S.; Hostetter, D. R.; Tajon, C.; Craik, C. S.; Alivisatos, A. P. Continuous Imaging of Plasmon Rulers in Live Cells Reveals Early-Stage Caspase-3 Activation at the Single-Molecule Level. *Proc. Natl. Acad. Sci. U. S. A.* **2009**, *106*, 17735–17740.
- (11) Maier, S. A.; Brongersma, M. L.; Kik, P. G.; Atwater, H. A. Observation of Near-Field Coupling in Metal Nanoparticle Chains Using Far-Field Polarization Spectroscopy. *Phys. Rev. B* **2002**, *65*193408.
- (12) Arnold, M. D.; Blaber, M. G.; Ford, M. J.; Harris, N. Universal Scaling of Local Plasmons in Chains of Metal Spheres. *Opt. Express* **2010**, *18*, 7528–7542.
- (13) Harris, N.; Arnold, M. D.; Blaber, M. G.; Ford, M. J. Plasmonic Resonances of Closely Coupled Gold Nanosphere Chains. *J. Phys. Chem. C* **2009**, *113*, 2784–2791.
- (14) Gunnarsson, L.; Rindzevicius, T.; Prikulis, J.; Kasemo, B.; Kall, M.; Zou, S. L.; Schatz, G. C. Confined Plasmons in Nanofabricated Single Silver Particle Pairs: Experimental Observations of Strong Interparticle Interactions. *J. Phys. Chem. B* **2005**, *109*, 1079–1087.
- (15) Jain, P. K.; El-Sayed, M. A. Surface Plasmon Coupling and Its Universal Size Scaling in Metal Nanostructures of Complex Geometry: Elongated Particle Pairs and Nanosphere Trimers. *J. Phys. Chem. C* **2008**, *112*, 4954–4960.
- (16) Tabor, C.; Murali, R.; Mahmoud, M.; El-Sayed, M. A. On the Use of Plasmonic Nanoparticle Pairs as a Plasmon Ruler: The Dependence of the Near-Field Dipole Plasmon Coupling on Nanoparticle Size and Shape. *J. Phys. Chem. A* **2009**, *113*, 1946–1953.
- (17) Ben, X.; Park, H. S. Size Dependence of the Plasmon Ruler Equation for Two-Dimensional Metal Nanosphere Arrays. *J. Phys. Chem. C* **2011**, *115*, 15915–15926.
- (18) Encina, E. R.; Coronado, E. A. Plasmon Coupling in Silver Nanosphere Pairs. *J. Phys. Chem. C* **2010**, *114*, 3918–3923.
- (19) Yang, L.; Wang, H.; Yan, B.; Reinhard, B. M. Calibration of Silver Plasmon Rulers in the 1–25 nm Separation Range: Experimental Indications of Distinct Plasmon Coupling Regimes. *J. Phys. Chem. C* **2010**, *114*, 4901–4908.
- (20) Garcia de Abajo, F. J. Optical Excitations in Electron Microscopy. *Rev. Mod. Phys.* **2010**, *82*, 209–275.
- (21) Nelayah, J.; Kociak, M.; Stephan, O.; Garcia de Abajo, F. J.; Tence, M.; Henrard, L.; Taverna, D.; Pastoriza-Santos, I.; Liz-Marzan, L. M.; Colliex, C. Mapping Surface Plasmons on a Single Metallic Nanoparticle. *Nat. Phys.* **2007**, *3*, 348–353.
- (22) Koh, A. L.; Bao, K.; Khan, I.; Smith, W. E.; Kothleitner, G.; Nordlander, P.; Maier, S. A.; McComb, D. W. Electron Energy-Loss Spectroscopy (EELS) of Surface Plasmons in Single Silver Nanoparticles and Dimers: Influence of Beam Damage and Mapping of Dark Modes. *ACS Nano* **2009**, *3*, 3015–3022.
- (23) Guiton, B. S.; Iberi, V.; Li, S.; Leonard, D. N.; Parish, C. M.; Kotula, P. G.; Varela, M.; Schatz, G. C.; Pennycook, S. J.; Camden, J. P. Correlated Optical Measurements and Plasmon Mapping of Silver Nanorods. *Nano Lett.* **2011**, *11*, 3482–3488.
- (24) de Lasson, J. R.; Mork, J.; Kristensen, P. T. Three-Dimensional Integral Equation Approach to Light Scattering, Extinction Cross Sections, Local Density of States, and Quasi-Normal Modes. *J. Opt. Soc. Am. B* **2013**, *30*, 1996–2007.
- (25) Rakic, A. D.; Djurisic, A. B.; Elazar, J. M.; Majewski, M. L. Optical Properties of Metallic Films for Vertical-Cavity Optoelectronic Devices. *Appl. Opt.* **1998**, *37*, 5271–5283.
- (26) Collins, S. M.; Midgley, P. A. Surface Plasmon Excitations in Metal Spheres: Direct Comparison of Light Scattering and Electron Energy-Loss Spectroscopy by Modal Decomposition. *Phys. Rev. B* **2013**, *87*, 235432.
- (27) Toscano, G.; Raza, S.; Jauho, A.-P.; Mortensen, N. A.; Wubs, M. Modified Field Enhancement and Extinction by Plasmonic Nanowire Dimers due to Nonlocal Response. *Opt. Express* **2012**, *20*, 4176–4188.
- (28) Esteban, R.; Borisov, A. G.; Nordlander, P.; Aizpurua, J. Bridging Quantum and Classical Plasmonics with a Quantum-Corrected Model. *Nat. Commun.* **2012**, *3*, 3825.
- (29) Kadkhodazadeh, S.; Wagner, J. B.; Kneipp, H.; Kneipp, K. Coexistence of Classical and Quantum Plasmonics in Large Plasmonic Structures with Subnanometer Gaps. *Appl. Phys. Lett.* **2013**, *103*083103.
- (30) Batson, P. E.; Reyes-Coronado, A.; Barrera, R. G.; Rivacoba, A.; Echenique, P. M.; Aizpurua, J. Nanoparticle Movement: Plasmonic Forces and Physical Constraints. *Ultramicroscopy* **2012**, *123*, 50–58.
- (31) Brongersma, M. L.; Hartman, J. W.; Atwater, H. A. Electromagnetic Energy Transfer and Switching in Nanoparticle Chain Arrays below the Diffraction Limit. *Phys. Rev. B* **2000**, *62*, 16356–16359.
- (32) Ruppini, R. Surface Modes of 2 Spheres. *Phys. Rev. B* **1982**, *26*, 3440–3444.
- (33) Nordlander, P.; Oubre, C.; Prodan, E.; Li, K.; Stockman, M. I. Plasmon Hybridization in Nanoparticle Dimers. *Nano Lett.* **2004**, *4*, 899–903.
- (34) Engheta, N.; Salandrino, A.; Alu, A. Circuit Elements at Optical Frequencies: Nanoinductors, Nanocapacitors, and Nanoresistors. *Phys. Rev. Lett.* **2005**, *95*, 095504.
- (35) Alu, A.; Engheta, N. Hertzian Plasmonic Nanodimer as an Efficient Optical Nanoantenna. *Phys. Rev. B* **2008**, *78*, 195111.
- (36) Johnson, P.; Christy, R. Optical Constants of Noble Metals. *Phys. Rev. B* **1972**, *6*, 4370–4379.